Infrastructure and Environment Scotland 3rd Postgraduate Conference
9th December 2015
Heriot-Watt University, Edinburgh

A Partition of Unity Boundary Element Method for Transient Wave Propagation

David Stark[1], Heiko Gimperlein[2]
Maxwell Institute for Mathematical Sciences and Department of Mathematics
Heriot-Watt University, Edinburgh[1,2]
Institute for Mathematics, University of Paderborn, Warburger, Str. 100, 33098 Paderborn, Germany[2]
(e-mail: ds221@hw.ac.uk)[1]

ABSTRACT

We propose a time-domain partition of unity boundary element method for wave propagation problems at high frequency. Travelling waves are included as enrichment functions into a time-domain boundary element solver. A major problem is the numerically-accurate set-up of the Galerkin matrix. We present preliminary numerical results of this method, discuss algorithmic aspects involved, and comment on relevant engineering applications.

1. INTRODUCTION

Boundary element methods (BEM) provide an efficient and extensively analyzed numerical scheme for time-independent or time-harmonic scattering and emission problems. In recent years, they have been explored for the simulation of transient phenomena, such as modeling of environmental noise [1] or electromagnetic scattering [2,3]. Further classical applications arise in computational and fluid mechanics. In terms of numerical methods, time-dependant boundary element methods were introduced by Bamberger and Ha-Duong [9]. The numerical implementation of the resulting marching-on-in-time schemes have since been extensively investigated especially in the French numerical community [2], with fast collocation methods developed for applications [3]. Adaptive mesh refinement methods have been explored recently [4]. See also [3,4] for some mathematical background.

Unlike finite element discretisations, BEM has the advantage of reducing the computation from the three dimensional domain to its two-dimensional boundary. Solving an integral equation on this boundary, the entire sound pressure field can be evaluated at any point in space even for the unbounded domains of scattering problems. With the FEM, one necessarily needs to mesh and possibly truncate the whole computational domain.

On the other hand, for time-harmonic wave propagation partition-of-unity finite and boundary element methods (PUFEM / PUBEM) have emerged as a practically efficient solution to deal with the rapid oscillations and numerical pollution at high wave numbers [5,6,7]. Enriched with local solutions to the Helmholtz equation, such discretisations considerably reduce the number of degrees of freedom to achieve engineering accuracy, as compared to standard FEM and BEM: The nature of the exact solution is encoded in the ansatz functions of the numerical method. In special situations, a careful choice of the enrichment functions leads to numerical methods whose performance is independent of the frequency.

In this work we introduce a time-domain partition-of-unity boundary element method. It extends the above works for time-harmonic wave propagation to truly transient problems in space and time. Practically, it includes plane-wave enrichment functions into the h-version time-domain boundary element procedure. It is the first work on enriched methods for time-dependent integral equation methods.

A main challenge is the accurate assembly of the Galerkin matrix. Using the quadrature method described in [8], we propose a carefully-chosen plane-wave enrichment and provide a preliminary numerical analysis of this scheme. The theoretical analysis of [2,9] proves that our method is stable and converges.

As for the structure of this article: In Section 2 we recall the initial-boundary problem for the acoustic wave equation which we consider and reformulate it as an integral formulation on the boundary of the scatterer. The partition-of-unity TDBEM is introduced in Section 3 and shown to lead to an explicit time-stepping scheme. Section 4 provides some details on the computation of the Galerkin matrix. After discussing different notions of convergence and error in Section 5, Section 6 presents preliminary numerical results for both the partition-of-unity method and the h-method obtained by turning off the enrichment. The results are put into perspective in Section 7.

2. THE WAVE EQUATION AND ITS INTEGRAL FORMULATION

We consider transient sound radiation problems in the exterior of a scatterer Ω^-, where Ω^- is a bounded polygon with connected complement $\Omega := \Omega^+ = \mathbb{R}^3 \setminus \Omega^-$. Let **n** be the outer normal vector on the boundary $\Gamma := \partial\Omega$.

Figure 1. Ω^- and outer normal **n**.

The acoustic pressure field $u(t,\mathbf{x})$ induced by an incident field u^{inc} from the exterior domain or from sources on Γ, fulfills the linear wave equation:

$$\frac{1}{c^2}\frac{\partial^2 u(t,\mathbf{x})}{\partial t^2} - \Delta u(t,\mathbf{x}) = 0 \tag{1}$$

where $\mathbf{x} \in \Omega$, $t \in \mathbb{R}$ and c is the wave velocity. We always set c=1 to simplify the notation.

We impose the initial conditions:

$$u(0,\mathbf{x}) = \frac{\partial}{\partial t}u(0,\mathbf{x}) = 0 \qquad \text{for } \mathbf{x} \in \Omega \tag{2}$$

and boundary conditions:

$$u(t,\mathbf{x}) = f(t,\mathbf{x}) \qquad \text{in } \mathbb{R} \times \Gamma. \tag{3}$$

We can represent the solution to the Dirichlet problem using a single-layer ansatz for $\mathbf{x} \notin \Gamma$:

$$u(t,\mathbf{x}) = \frac{2}{4\pi}\int_\Gamma \frac{\phi(t-|\mathbf{x}-\mathbf{y}|,\mathbf{y})}{|\mathbf{x}-\mathbf{y}|}\, ds_y \tag{4}$$

The single-layer operator is continuous when passing with **x** to the boundary, hence (3) yields the boundary integral equation:

$$V\phi(t,\mathbf{x}) = f(t,\mathbf{x}) \tag{5}$$

for the single layer operator:

$$V\phi(t,\mathbf{x}) = \frac{2}{4\pi}\int_\Gamma \frac{\phi(t-|\mathbf{x}-\mathbf{y}|,\mathbf{y})}{|\mathbf{x}-\mathbf{y}|}\, ds_y. \tag{6}$$

Multiplying (6) by the time derivative of a test function Ψ and integrating over Γ, a coercive weak formulation of the integral equation is:

$$\int_0^\infty \exp(-2\sigma t)\int_\Gamma (V\phi(t,\mathbf{x}))\dot{\psi}(t,\mathbf{x})\, ds_x dt = \int_0^\infty \exp(-2\sigma t)\int_\Gamma f(t,\mathbf{x})\dot{\psi}(t,\mathbf{x})\, ds_x dt \tag{7}$$

In later computations we set $\sigma = 0$ [2,8].

3.PARTITION OF UNITY TDBEM

We use a time-dependent boundary element method to solve (7). A numerical approximation is sought of the form:

$$\phi = \sum c_j \phi_j \tag{8}$$

where φ_j are suitable basis functions in space and time. We denote the space of all such functions S.

We use a plane wave basis enrichment to better approximate the oscillatory nature of solutions at large frequency. In the frequency domain, such partition-of-unity methods are discussed by Trevelyan et al. in [5,6] for boundary elements, and in [7] for finite elements.

A first work by Ham and Bathe in the time-domain [10] discusses the enrichment for wave propagation problems in two dimensions. They choose φ_j as:

$$\phi_i = \widetilde{\Lambda}_i(t)\Lambda_i(\mathbf{x})\cos(\omega_i t - \mathbf{k}_i \mathbf{x}_i + \sigma_i) \tag{9}$$

where $\Lambda_j(t)$ is a piecewise polynomial hat function in space, and $\Lambda_i(\mathbf{x})$ a corresponding hat function in space. **K** denotes the spatial and ω the temporal frequency $\omega = |\mathbf{k}|$ of the plane wave. $\sigma_i \in \{0, \pi/2\}$ allows to include both sine and cosine enrichments.

We use the basis functions (9) in a partition-of-unity TDBEM in 3 dimensions, with both piecewise constant shape functions $\Lambda_j(t)$ and $\Lambda_i(\mathbf{x})$. We also use piecewise linear shape functions in time. The resulting discretised numerical scheme for the Dirichlet problem (7) is:

Find $\varphi_{h,\Delta t}$ such that for all $\Psi_{h,\Delta t} \in$ S:

$$\langle V\phi_{h,\Delta t}, \dot{\psi}_{h,\Delta_t}\rangle = \langle f, \dot{\psi}_{h,\Delta_t}\rangle \tag{10}$$

Because of the piecewise constant shape functions, the space-time equation (10) takes a lower triangular form, where each block corresponds to one time step.

$$\begin{array}{c|c} & \xleftrightarrow{\quad t_m \quad} \\ \hline \updownarrow t_n & \begin{pmatrix} \mathbf{V}^0 & 0 & 0 & 0 \\ \mathbf{V}^1 & \mathbf{V}^0 & 0 & 0 \\ \mathbf{V}^2 & \mathbf{V}^1 & \mathbf{V}^0 & 0 \\ \mathbf{V}^3 & \mathbf{V}^2 & \mathbf{V}^1 & \mathbf{V}^0 \end{pmatrix} \end{array} \begin{pmatrix} \mathbf{c}_1 \\ \mathbf{c}_2 \\ \mathbf{c}_3 \\ \mathbf{c}_4 \end{pmatrix} = \begin{pmatrix} \mathbf{f}_1 \\ \mathbf{f}_2 \\ \mathbf{f}_3 \\ \mathbf{f}_4 \end{pmatrix} \updownarrow t_n$$

Figure 2. The "Marching on in Time" (MOT) matrix system.

The matrix $\mathbf{V}^j$ and right hand side $\mathbf{f}_j$ are calculated at time t_j. The solution vector $\mathbf{c}_j$ gives the coefficients in (8) at time t_j. More explicitly:

$\mathbf{V}^0\mathbf{c}_1 = \mathbf{f}_1$
$\mathbf{V}^0\mathbf{c}_2 = \mathbf{f}_2 - \mathbf{V}^1\mathbf{c}_1$
$\mathbf{V}^0\mathbf{c}_3 = \mathbf{f}_3 - \mathbf{V}^2\mathbf{c}_1 - \mathbf{V}^1\mathbf{c}_2 \ldots$

Solving the system in this way, is a "marching on in time" (MOT) algorithm for time-stepping.

In each time step, we solve a block-linear algebraic system as below:

$$\begin{array}{c|ccc} & k_1 & k_2 & k_3 \\ \hline k_1 & & & \\ k_2 & & & \\ k_3 & & & \end{array} \begin{pmatrix} \mathbf{V}_{11} & \mathbf{V}_{12} & \mathbf{V}_{13} \\ \mathbf{V}_{21} & \mathbf{V}_{22} & \mathbf{V}_{23} \\ \mathbf{V}_{31} & \mathbf{V}_{32} & \mathbf{V}_{33} \end{pmatrix} \begin{pmatrix} \mathbf{c}_1 \\ \mathbf{c}_2 \\ \mathbf{c}_3 \end{pmatrix} = \begin{pmatrix} \mathbf{f}_1 \\ \mathbf{f}_2 \\ \mathbf{f}_3 \end{pmatrix} \begin{array}{c} k_1 \\ k_2 \\ k_3 \end{array}$$

Figure 3. The PUBEM system for each time step.

Each $\mathbf{V}_{mn}$ is a matrix of size (#nodes) x (#nodes), which relates to two **k** vectors - one for the ansatz function φ, and one for the test function Ψ. These **k** are determined by the row and column number of each matrix. For example, matrix $\mathbf{V}_{21}$ relates to $\mathbf{k}_2$ (taken from the row, and used in the test function) and $\mathbf{k}_1$ (taken from the column, and used in the ansatz function).

The numerical scheme (10) minimises the energy:

$$E := \frac{1}{2}\phi \cdot (\mathbf{V}\phi) - F \cdot \phi \tag{11}$$

As a Galerkin method, the stability and convergence of the numerical method (10) are guaranteed [9,2].

4. ALGORITHMIC ASPECTS

Up to a constant pre-factor, as in [8] each element of the Galerkin matrix $\mathbf{V}_{m,n}$ is given by:

$$V_{m,n} := \int_0^\infty \int_\Gamma \underbrace{\int_\Gamma \frac{\phi_m(t-|\mathbf{x}-\mathbf{y}|,\mathbf{y})}{|\mathbf{x}-\mathbf{y}|}\, dS_y}_{V\phi} \quad \dot{\psi}_n(t,\mathbf{x})\, dS_x \quad dt \tag{12}$$

We first evaluate the time integral analytically, resulting in an analytic expression for $\mathbf{V}_{m,n}$ which has the form:

$$\begin{aligned} V_{m,n} = \int_\Gamma \int_\Gamma \frac{1}{|\mathbf{x}-\mathbf{y}|}\Lambda_m(\mathbf{y})\Lambda_n(\mathbf{x})\Big\{ & \\ F_1(\mathbf{y},\mathbf{x},\omega_m,\omega_n)\cdot &\ \cos(\mathbf{k}_m\cdot\mathbf{y})\cos(\mathbf{k}_n\cdot\mathbf{x}) \\ +F_2(\mathbf{y},\mathbf{x},\omega_m,\omega_n)\cdot &\ \cos(\mathbf{k}_m\cdot\mathbf{y})\sin(\mathbf{k}_n\cdot\mathbf{x}) \\ -F_3(\mathbf{y},\mathbf{x},\omega_m,\omega_n)\cdot &\ \cos(\mathbf{k}_m\cdot\mathbf{y})\omega_n\cos(\mathbf{k}_n\cdot\mathbf{x}) \\ +F_4(\mathbf{y},\mathbf{x},\omega_m,\omega_n)\cdot &\ \cos(\mathbf{k}_m\cdot\mathbf{y})\omega_n\sin(\mathbf{k}_n\cdot\mathbf{x}) \\ +F_5(\mathbf{y},\mathbf{x},\omega_m,\omega_n)\cdot &\ \sin(\mathbf{k}_m\cdot\mathbf{y})\cos(\mathbf{k}_n\cdot\mathbf{x}) \\ +F_6(\mathbf{y},\mathbf{x},\omega_m,\omega_n)\cdot &\ \sin(\mathbf{k}_m\cdot\mathbf{y})\sin(\mathbf{k}_n\cdot\mathbf{x}) \\ -F_7(\mathbf{y},\mathbf{x},\omega_m,\omega_n)\cdot &\ \sin(\mathbf{k}_m\cdot\mathbf{y})\omega_n\cos(\mathbf{k}_n\cdot\mathbf{x}) \\ +F_8(\mathbf{y},\mathbf{x},\omega_m,\omega_n)\cdot &\ \sin(\mathbf{k}_m\cdot\mathbf{y})\omega_n\sin(\mathbf{k}_n\cdot\mathbf{x})\Big\}\, dS_y\, dS_x \end{aligned} \tag{13}$$

The functions F_j vanish outside a light cone – a spherical shell whose inner and outer radii relate to the time steps t_m *and* t_n, see Figure 4:

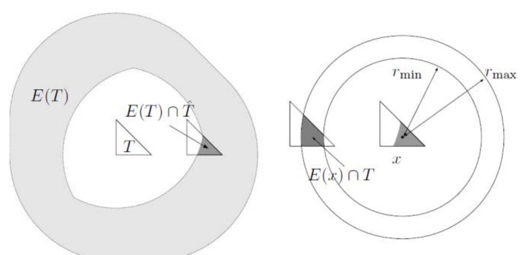

Figure 4. Light cone and domain of influence [8].

Here, triangle T is the ansatz element, and triangle T is the test element. The rightmost diagram shows the light cone around a point **x** in T represents the inner integral in (13). The leftmost diagram shows the union of all light cones around points in T, as needed for the outer integral in (13).

Because of the denominator |**x**-**y**| in (12) and the singularities of F_j at the boundary of the light cone, a main challenge in the TDBEM is the accurate computation of the matrix elements $\mathbf{V}_{m,n}$.

For the inner integration (shown on the right in Figure 4), we consider the grey area on triangle T.

We first project the point of observation **x** onto the ansatz triangle plane, as shown in Figure 5.

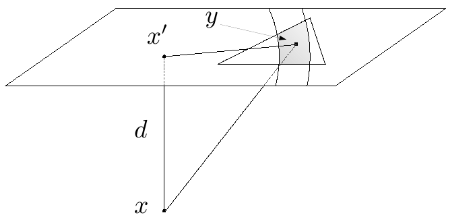

Figure 5. The projection of **x** onto the triangle plane, which we call **x**' [8].

In the two-dimensional plane, we change to polar coordinates around **x**' and partition the region into sectors D_l as in Figure 6.

$$(P\phi)(\mathbf{x}) := \sum_{l=1}^{n_d} \int_{D_l} \frac{\phi(\mathbf{y})}{|d^2+r^2|} \; ds_y. \tag{14}$$

where $d = |\mathbf{x}\text{-}\mathbf{x}'|$. The integrals over D_l have simple descriptions in polar coordinates and may be accurately evaluated with a geometrically graded hp-Gauss quadrature [8].

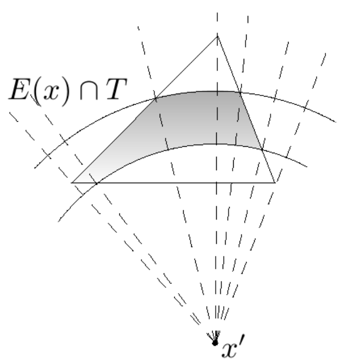

Figure 6. A partitioned element/light cone intersection, in polar coordinates [8].

5. MEASURING THE ERROR

We quantify the numerical errors in three ways:

1. By comparing $\varphi_{h,\,\Delta t}$ to the density obtained from standard h-TDBEM with a fine mesh.
2. By comparing $u_{h,\,\Delta t}$ to the sound pressure from standard h-TDBEM with a fine mesh.
3. By considering the energy (see below).

The first two methods require varying degrees of post-processing. We compute $\varphi_{h,\,\Delta t}$ from formulas (8) and (9). To compute $u_{h,\,\Delta t}$ requires more work:

The condition:

$$t_i \quad \leq \quad \big[t - |\mathbf{x}-\mathbf{y}|\big] \quad \leq \quad t_{i+1} \tag{15}$$

generally holds for some time step i. For a linear basis in time, we use the linear interpolation formula to compute φ at retarded times:

$$\begin{aligned}\phi_j(t-|\mathbf{x}-\mathbf{y}|,\mathbf{y}) = \sum_{h=1}^{N_h}\Bigg\{ & C_{i,j}\Bigg[1-\Bigg(\frac{\big[t-|\mathbf{x}-\mathbf{y}|\big]-t_i}{t_{i+1}-t_i}\Bigg)\Bigg] \\ & \cos\big(\omega_h\big[t-t_i-|\mathbf{x}-\mathbf{y}|\big]-\mathbf{k}_h\cdot\mathbf{y}+\sigma_h\big)\Lambda_j(\mathbf{y}) \\ & + C_{i+1,j}\Bigg(\frac{\big[t-|\mathbf{x}-\mathbf{y}|\big]-t_i}{t_{i+1}-t_i}\Bigg) \\ & \cos\big(\omega_h\big[t-t_{i+1}-|\mathbf{x}-\mathbf{y}|\big]-\mathbf{k}_h\cdot\mathbf{y}+\sigma_h\big)\Lambda_j(\mathbf{y})\Bigg\}\end{aligned} \tag{16}$$

where i indexes the time step, j indexes the element, and h indexes the enrichment functions. The position vector **y** is the spatial Gauss point where the function is evaluated on the element, and **x** is a point of evaluation outside Γ, where u is to be evaluated from.

We can now use this to calculate u:

$$\begin{aligned}u(t,\mathbf{x}) &= \frac{2}{4\pi}\int_\Gamma \frac{\phi(t-|\mathbf{x}-\mathbf{y}|,\mathbf{y})}{|\mathbf{x}-\mathbf{y}|}\,ds_y \\ &= \frac{2}{4\pi}\sum_{i=1}^{N}\int_{E(\mathbf{x})_i}\frac{\phi(t-|\mathbf{x}-\mathbf{y}|,\mathbf{y})}{|\mathbf{x}-\mathbf{y}|}\,ds_y \\ &= \frac{2}{4\pi}\sum_{i=1}^{N} J(E(\mathbf{x})_i)\sum_{j=1}^{15}\frac{\phi(t-|\mathbf{x}-\mathbf{p}_j|,\mathbf{p}_j)}{|\mathbf{x}-\mathbf{p}_j|}\end{aligned} \tag{17}$$

where we decompose Γ into its natural covering of elements and use a projection to the reference triangle to calculate the Gauss points $\mathbf{p}_j$ on the reference triangle. $J(E(\mathbf{x})_i)$ is the Jacobian for element $E(\mathbf{x})_i$.

A Galerkin method seeks a minimiser for the corresponding energy functional, here given by

$$E := \frac{1}{2}\phi\cdot(\mathbf{V}\phi) - F\cdot\phi \tag{18}$$

V is the full space-time Galerkin matrix, and F the full space-time right hand side vector. We compute each part component-wise,

$$\mathbf{V}\phi = \begin{bmatrix} \mathbf{V}^0\phi^0 \\ \mathbf{V}^1\phi^0+\mathbf{V}^0\phi^1 \\ \mathbf{V}^2\phi^0+\mathbf{V}^1\phi^1+\mathbf{V}^0\phi^2 \\ etc... \end{bmatrix} \tag{19}$$

and

$$F\phi = F^0\cdot\phi^0 + F^1\cdot\phi^1 + F^2\cdot\phi^2 + ... \tag{20}$$

where numerals index the time steps.

6. PRELIMINARY NUMERICAL RESULTS

To analyse the convergence of our algorithm, we first consider a wave problem with known exact solution φ when Γ is the sphere of radius 1. If $f(t,\mathbf{x}) = \sin(t)^5$, $\varphi(t) = 5\sin(t)^4 \cos(t)$ (for $t < 2$) [11].

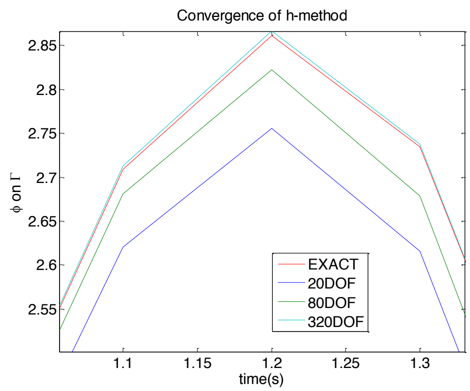

Figure 7. Convergence everywhere, as we increase the degrees of freedom, for *t*<2s.

Figure 7 shows the numerical results for $\varphi_{h,\Delta t}$ with 20, 80 resp. 320 triangles and constant ratio of *h* and the time step for our implementation of the partition-of-unity TDBEM, with **k**=0.

A plot of degrees of freedom vs. the absolute error in the centroid of a triangle is shown in Figure 8. We thereby recover the convergence of h-TDBEM, with almost linear order of convergence.

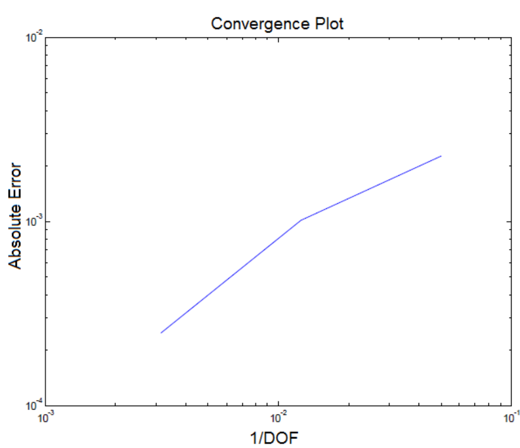

Figure 8. The absolute error at *t* = 1.2s.

The following plot shows some preliminary results for the piecewise linear shape functions in time with enrichment |**k**|>0.

For Γ, a regular convex icosahedron (20 triangular faces) of diameter 2 and centered in (0, 0, 0), we use the right hand side: $f(t,x)=\exp(-4/t^2)\cos(\omega_f t-\mathbf{k}_f\mathbf{x})$, a plane wave with $\mathbf{k}_f=(1, 0.5, 0.1)$ which is smoothly turned on for small times. An h-TDBEM approximation with 320 triangles serves as replacement for an 'exact' solution. We compare with a partition-of-unity TDBEM based on 20 triangles and *n* enrichment functions in each triangle. The approximations $\varphi_{h,\Delta t}$ and $u_{h,\Delta t}$ show similar convergence. Figure 9 shows the numerical PU-TDBEM solution for the sound pressure $u_{h,\Delta t}$ in the point (1.2, 0.5, 0.4) outside Γ.

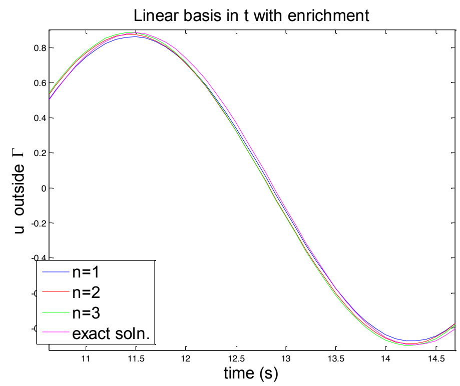

Figure 9. Plot of *u vs t* with our linear basis, using a varying number of enrichment functions.

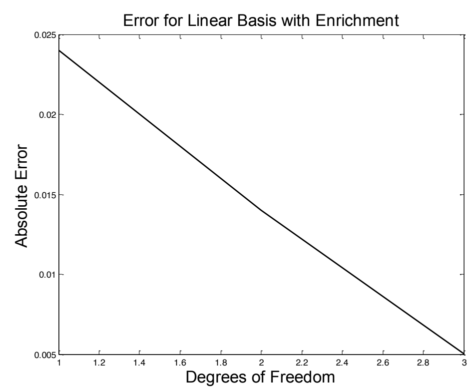

Figure 10. Plot of absolute error vs degrees of freedom for the linear basis. Taken at *t* = 11.6s.

The corresponding absolute errors are exhibited in Figure 10.

7. CONCLUSIONS AND OUTLOOK

This work presents a first step towards enriched time-domain methods, here for boundary elements. Even for finite elements such methods are just beginning to be explored in time-domain. They present a promising approach to take large time steps even for rapidly oscillating solutions, with applications from imaging to the numerics of concert halls.

Our plots indicate that we have implemented a partition-of-unity method which converges for low numbers of suitably chosen enrichment functions.

We hope to extend our numerical experiments to more realistic geometries and data, where 20 or more enrichment functions would be required. For large numbers of enrichments the Galerkin matrix is known to be badly conditioned for time-independent problems.

One motivation comes from the sound radiation of truck tyres [1]. Here, the boundary of the tyre is meshed and treated as an emitter. Figure 9 shows snapshots from the corresponding time evolution.

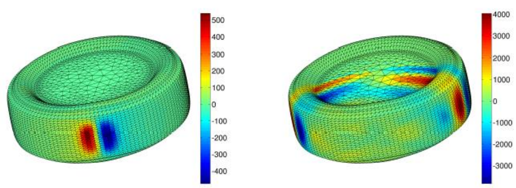

Figure 9. Time evolution of the density for a vibrating tyre [1].

A longer-term outlook might compare a working time-domain PUBEM method with hp-adaptivity as competing approaches to deal with numerical pollution at high frequency.

REFERENCES

[1] L. Banz, H. Gimperlein, Z. Nezhi, E. P. Stephan, Time domain BEM for sound radiation of tires, preprint.

[2] T. Ha Duong. On retarded potential boundary integral equations and their discretisations. Topics in computational wave propagation, Lect. Notes Comput. Sci. Eng., Vol. 31 (2003). Springer: Berlin, 301-336.

[3] A. E. Yilmaz, J.-M. Jin, E. Michielssen, Time domain adaptive integral method for surface integral equations, IEEE Trans. Antennas Propagation **52** (2004); 2692-2708.

[4] H. Gimperlein, M. Maischak, E. P. Stephan, Adaptive time-domain boundary element methods and engineering applications, invited survey, Journal of Integral Equations and Applications, to appear (2016).

[5] E. Perrey-Debain, J. Trevelyan, P. Bettess, Wave Boundary Elements: A Theoretical Overview Presenting Applications in Scattering of Short Waves, Engineering Analysis with Boundary Elements 28 (2004) 131-141.

[6] E. Perrey-Debain, J. Trevelyan, P. Bettess, On Wave Boundary Elements for Radiation and Scattering, IEEE Transactions on Antennas and Propagation, vol. 53, no. 2, (Feb 2005).

[7] O. Laghrouche, P. Bettess, E. Perrey-Debain, J. Trevelyan, Wave Interpolation Finite Elements for Helmholtz Problems with Jumps in the Wave Speed, Comput. Methods Appl. Mech. Engrg. 194 (2005) 367-381.

[8] E. Ostermann, Numerical Methods for Space-Time Variational Formulations of Retarded Potential Boundary Integral Equations, Ph.D. thesis, Leibniz Universität Hannover, 2009.

[9] A. Bamberger, T. Ha Duong, Formulation variationnelle espace-temps pour le calcul par potentiel retard de la diffraction d'une onde acoustique. Math. Methods in the Appl. Sciences 8 (1986); 405-435 and 598-608.

[10] S. Ham, K.J. Bathe, A Finite Element Method Enriched For Wave Propagation Problems, Computers And Structures 94-95 (2012), 1-12.

[11] S. Sauter, A. Veit, Retarded boundary integral equations on the sphere: exact and numerical solution, IMA J. Numer. Anal. 34 (2014); 675-699.